Reaction of Phenyl Radicals with Propyne

ARTICLE *in* JOURNAL OF THE AMERICAN CHEMICAL SOCIETY · APRIL 2002

Impact Factor: 12.11 · DOI: 10.1021/ja017018+ · Source: PubMed

J|A|C|S
ARTICLES
Published on Web 02/19/2002

Reaction of Phenyl Radicals with Propyne

Luc Vereecken,*,† Jozef Peeters,† Holger F. Bettinger,‡ Ralf I. Kaiser,§ Paul v. R. Schleyer,||,⊥ and Henry F. Schaefer, III||

Contribution from the Department of Chemistry, University of Leuven, Celestijnenlaan 200F, B-3001 Heverlee, Belgium; Lehrstuhl für Organische Chemie II, Ruhr-Universität Bochum, 44780 Bochum, Germany; Department of Chemistry, University of York, York YO10 5DD, U.K.; and Center for Computational Quantum Chemistry, University of Georgia, Athens, Georgia 30602

Received September 6, 2001. Revised Manuscript Received December 7, 2001

Abstract: The potential energy surface (PES) for the phenyl + propyne reaction, which might contribute to the growth of polycyclic aromatic hydrocarbons (PAHs) under a wide variety of reaction conditions, is described. The PES was characterized at the B3LYP-DFT/6-31G(d) and B3LYP-DFT/6-311+G(d,p) levels of theory. The energies of the entrance transition states, a direct hydrogen-transfer channel and two addition reactions leading to chemically activated $C_9H_9^\dagger$ intermediates, were also evaluated at the QCISD(T)/6-311G(d,p) and CCSD(T)/6-311G(d,p) levels of theory. An extensive set of unimolecular reactions was examined for these activated $C_9H_9^\dagger$ intermediates, comprising 70 equilibrium structures and over 150 transition states, and product formation channels leading to substituted acetylenes and allenes such as PhCCH, $PhCCCH_3$, and $PhCHCCH_2$ were identified. The lowest energy pathway leads to indene, a prototype PAH molecule containing a five-membered ring. The title reaction thus is an example of possible direct formation of a PAH containing a five-membered ring, necessary to explain formation of nonplanar PAH structures, from an aromatic radical unit and an unsaturated hydrocarbon bearing an odd number of carbons. Extensive Supporting Information is available.

I. Introduction

The reactions of phenyl radicals with unsaturated hydrocarbons have been proposed to be important for the formation of polycyclic aromatic hydrocarbons (PAHs) in a number of environments, ranging from the circumstellar envelopes of carbon-rich stars and the interstellar medium[1−3] to combustion processes.[4,5] PAHs and the related soot formation have been key issues in combustion chemistry for decades. The mechanisms of formation of complex, carbon-bearing molecules in the interstellar medium have also become an important topic recently, as some authors argue that about 20% of the cosmically available carbon is present as PAHs.[6−8] Photochemical reactions[9] of these PAHs on ice particles yield important organic compounds,[10] such as alcohols and ethers. The formation of these biologically relevant molecules in space in turn has implications for new theories[11] of biogenesis, which are based on the accretion of extraterrestrial prebiotic organic matter on earth: currently about 40000 tons appear to be accumulated annually.[12]

A detailed and complete understanding of the formation of PAH molecules requires systematic research to elucidate the basic elementary chemical reactions underlying the PAH growth processes. Chemical reaction networks[1−3] modeling the formation of PAHs in extraterrestrial environments suggest that benzene, phenyl radicals, and/or possibly cyclo-C_5H_5 radicals are crucial reaction intermediates. Likewise, in combustion systems it is generally accepted that formation of PAHs and soot particles starts from an aromatic species:[13] a benzene molecule or a phenyl radical. Most authors consider the combination of C_3H_3 and/or C_3H_2 entities as the principal source of this first aromatic ring,[14−18] in preference over older mechanisms[4,19] based on C_2H_2 and C_4H_x additions. For subsequent

* To whom correspondence should be addressed. E-mail: Luc.Vereecken@chem.kuleuven.ac.be.
† University of Leuven.
‡ Ruhr-Universität Bochum.
§ University of York.
|| University of Georgia.
⊥ Also at the Institut für Organische Chemie, Universität Erlangen-Nürnberg, Germany.

(1) Cherchneff, I.; Barker, J. R. *Astrophys. J.* **1992**, *394*, 703.
(2) Messenger, S.; Amari, S.; Gao, X. *Astrophys. J.* **1998**, *502*, 284.
(3) Allain, T.; Sedlmayr, E.; Leach, S. *Astron. Astrophys.* **1997**, *323*, 163.
(4) Frenklach, M.; Clary, D. W.; Gardiner, W. C.; Stein, S. E. *Symp. (Int.) Combust., [Proc.]* **1984**, *20*, 887.
(5) Kazakov, A.; Frenklach, M. *Combust. Flame* **1998**, *112*, 270.
(6) Allamandola, L. J.; Tielens, A.; Barker, J. R. *Astrophys. J., Suppl. Ser.* **1989**, *71*, 733.
(7) Schlemmer, S.; Cook, D. J.; Harrison, J. A.; Wurfel, B.; Chapman, W.; Saykally, R. J. *Science* **1994**, *265*, 1686.
(8) Boulanger, F.; Boissel, P.; Cesarsky, D.; Ryter, C. *Astron. Astrophys.* **1998**, *339*, 194.
(9) Allamandola, L. J.; Tielens, A.; Barker, J. R. In *Interstellar Processes*; Hollenbach, D. J., Thronson, H. A., Eds.; D. Reidel Publishing Co.: Dordrecht, The Netherlands, 1987; pp 471−489.
(10) Bernstein, M. P.; Sandford, S. A.; Allamandola, L. J.; Seb Gillette, J.; Clemett, S. J.; Zare, R. N. *Science* **1999**, *283*, 1135.
(11) Goldanskii, V. I. *J. Phys. Chem. A* **1997**, *101*, 3424.
(12) Love, S. D.; Brownlee, D. E. *Science* **1993**, *262*, 550.
(13) Kern, R. D.; Wu, C. H.; Yong, J. N.; Pamidimukkala, K. M.; Singh, H. J. *Energy Fuels* **1988**, *2*, 454.
(14) Wu, C.; Kern, R. *J. Chem. Phys.* **1987**, *91*, 6291.
(15) Alkemade, U.; Homann, K. Z. *Phys. Chem. Neue Folge* **1989**, *161*, 19.
(16) Melius, C. F.; Miller, J. A.; Evleth, E. M. *Symp. (Int.) Combust., [Proc.]* **1991**, *23*, 85.

PAH growth, the model beginning with a phenyl radical, proposed by Frenklach et al.,[4,5] currently seems to be the most favorable synthetic route, in both combustion and interstellar chemistry. This model proposes a sequential addition of acetylene molecules, C_2H_2, to the phenyl radical to form naphthalene-like PAH species. Surprisingly, no PAH-growth models seem to include the reactions of phenyl radicals with molecules bearing an odd number of carbons, despite the importance of C_3H_x species compared to acetylene in the formation of the first aromatic ring, and the observation that C_3H_x molecules are among the most abundant organic molecules observed in the interstellar medium.[20−24] In contrast to the Frenklach mechanism,[4,5] which leads mainly to planar, naphthalene-like PAHs consisting of (substituted) six-membered rings, addition of odd-numbered C_3H_x species to phenyl radicals could directly yield PAHs incorporating five-membered rings. These five-membered rings are necessary to explain formation of nonplanar PAH structures, such as the fullerenes observed in large quantities in soot deposits.[25] To our knowledge, no specific PAH molecules have yet been identified in space. Our understanding of PAH formation in the different reaction conditions could benefit from examining the impact of reactions of aromatic units with molecules bearing an odd number of carbons.

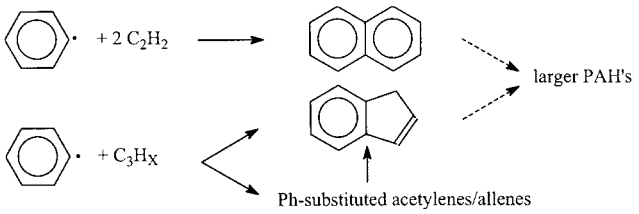

An important question that needs to be addressed is whether this class of reactions can contribute to PAH growth; i.e., can it compete with the phenyl + acetylene reactions used in the traditional PAH-growth models? Indeed, both in combustion systems and in dark interstellar clouds, acetylene is often present in comparatively high concentrations. In flames,[26−28] typical C_3H_4 concentrations are only a few percent of the acetylene concentration. However, transition-state theory calculations[29,30] at 1500 K predict rate coefficients for the Ph + C_3H_4 (propyne, allene) reaction that are about an order of magnitude higher than that for acetylene (8×10^{-13} cm^3 s^{-1}),[31] due to the effect of the degrees of freedom for internal rotation that are absent or less effective in the rigid, unsubstituted acetylene. Hence, the rate of reaction for phenyl with C_3H_4 should amount to a few tenths of that with acetylene. Likewise, the concentrations of C_3H_3 and C_3H_2 are roughly 3 orders of magnitude below those of acetylene, but as the reaction with phenyl are barrierless radical−radical/carbene reactions, rate coefficients close to the collision limit are expected ($\sim 10^{-10}$ cm^3 s^{-1}), i.e., about 2 orders of magnitude higher than for Ph + C_2H_2. Again, this leads to a sizable contribution of C_3H_x species in the phenyl consumption; the total reaction flux with C_3H_x isomers sums to only 2−5 times below that with acetylene. In the very low temperature regime found inside dark interstellar clouds, the nonzero activation barrier of the Ph + C_2H_2 reaction leads to negligible reaction rates, even for the very long reaction times available in space. Here, the fast, barrierless radical−radical/carbene reaction of Ph + C_3H_x ($x = 1-3$) will easily outrun the reaction with acetylene. The abundance of C_3H_x species is comparable to those of other observed potential reaction partners for phenyl[32−34] (excluding H and H_2, which are present in very high relative abundances and have a distinct role in aromatics formation[35]), such that C_3H_x molecules can be an important coreactant. Insufficient data are available for estimates pertaining to the very high temperature regime ($T \approx 4000$ K, very low pressures) in the outflow of carbon stars close to the photosphere. The stability of acetylene might result in high C_2H_2 concentrations compared to that of C_3H_x; on the other hand, the rate coefficients of the Ph + C_3H_x reactions seem to be higher at these temperatures,[36] such that these latter reactions cannot be excluded a priori.

From the above, it is clear that reactions of aromatic units with molecules bearing an odd number of carbons can be important reaction pathways. However, a crucial drawback of all current chemical models is the lack of well-defined input data, be it from experimental or theoretical sources. Although rate coefficients between 10^{-12} and 10^{-14} cm^3 s^{-1} have been measured for phenyl radical reactions with olefins and alkynes at temperatures up to 1100 K, and entrance barriers were determined to be 25−43 kJ mol^{-1}, the reaction products of most complex phenyl reactions are purely speculative.[37−40] This absence of detailed information also holds true for the title reaction, phenyl + propyne. This reaction was not proposed earlier as a possible source of PAH precursors, but it is a suitable representative of the class of reactions of aromatic units with molecules bearing an odd number of carbons; one of our reasons for choosing propyne as the first C_3H_x coreactant was its chemical similarity to acetylene. We have contributed to this research previously by a combined crossed molecular beams and computational study of the title reaction.[41] In this paper, we present a theoretical characterization of a large part of the

(17) Morter, C.; Farhat, S.; Adamson, J.; Glass, G.; Curl, R. *J. Phys. Chem.* **1994**, *98*, 7029.
(18) Miller, J. A.; Volponi, J. V.; Pauwels, J.-F. *Combust. Flame* **1996**, *105*, 451.
(19) Cole, J. A.; Bittner, J. D.; Longwell, J. P.; Howard, J. B. *Combust. Flame* **1984**, *56*, 51.
(20) Abramovich, R. A., Ed. *Reactive Intermediates*; Plenum: New York, 1980.
(21) Almond, M. J., Ed. *Short-lived Molecules*; Ellis Horwood: New York, 1990.
(22) Matthews, H.; Irvine, W. M. *Astrophys. J.* **1985**, *298*, L61.
(23) Thaddeus, P.; Vrtilek, J. M.; Gottlieb, C. A. *Astrophys. J.* **1985**, *299*, L63.
(24) Cernicharo, J.; Gottlieb, C. A.; Guélin, M.; Killian, T. C.; Paubert, G.; Thaddeus, P.; Vrtilek, J. M. *Astrophys. J.* **1991**, *368*, L39.
(25) Homann, K. *Angew. Chem., Int. Ed. Engl.* **1998**, *37*, 2435.
(26) Bittner, J. D.; Howard, J. *Symp. (Int.) Combust., [Proc.]* **1982**, *19*, 211.
(27) Castaldi, M. J.; Marinov, N. M.; Melius, C. F.; Huang, J.; Senkan, S. M.; Pitz, W. J.; Westbrook, C. K. *Symp. (Int.) Combust., [Proc.]* **1996**, *26*, 693.
(28) Bhargava, A.; Westmoreland, P. R. *Combust. Flame* **1998**, *113*, 333.
(29) Vereecken, L.; Bettinger, H.; Peeters, J. Reactions of chemically activated $C_9H_{9\dagger}$ species I: The product distribution of the reaction of phenyl radicals with propyne. *Phys. Chem. Chem. Phys.*, submitted for publication.
(30) Vereecken, L.; Peeters, J.; et al. Manuscripts in preparation.
(31) Yu, T.; Lin, M. C.; Melius, C. F. *Int. J. Chem. Kinet.* **1994**, *26*, 1095.
(32) Ohishi, M.; Irvine, W. M.; Kaifu, N. In *Astrochemistry of Cosmic Phenomena*; Singh, P. D., Ed.; 1992; Kluwer Academic Publishers, Dordrecht, The Netherlands, p 171.
(33) Lee, H.-H.; Bettens, R. P. A.; Herbst, E. *Astron. Astrophys., Suppl. Ser.* **1996**, *119*, 111.
(34) Terzieva, R.; Herbst, E. *Astrophys. J.* **1998**, *501*, 207.
(35) McEwan, M. J.; Scott, G. B. I.; Adams, N. G.; Babcock, L. M.; Terzieva, R.; Herbst, E. *Astrophys. J.* **1999**, *513*, 287.
(36) Yu, T.; Lin, M. C.; Melius, C. F. *Int. J. Chem. Kinet.* **1994**, *26*, 1095.
(37) Duncan, F. J.; Trotman-Dickenson, A. F. *J. Chem. Soc.* **1962**, *52*, 4672.
(38) Fahr, A.; Stein, S. E. *Symp. (Int.) Combust., [Proc.]* **1989**, *52*, 1023.
(39) Herzler, J.; Frank, P. *Ber. Bunsen-Ges. Phys. Chem.* **1992**, *96*, 1333.
(40) Yu, T.; Lin, M. *Combust. Flame* **1995**, *100*, 169.
(41) Kaiser, R. I.; Asvany, O.; Lee, Y. T.; Bettinger, H. F.; Schleyer, P. v. R.; Schaefer, H. F. *J. Chem. Phys.* **2000**, *112*, 4994.

potential energy surface (PES) of the reaction of phenyl radicals (C_6H_5) with propyne (C_3H_4), showing that the energetically most favorable reaction channel leads to indene and that this reaction channel is accessible to all chemically activated intermediates formed initially, even at very low temperatures. Subsequent papers[29,30] will focus on the rate constants and product distributions of reactions which proceed over this PES by theoretical-kinetic analyses. These latter papers will concern not only the reaction of phenyl radicals with propyne, but also those of phenyl + allene and cyclopropene, and $PhCH_2 + C_2H_2$, which all proceed over this C_9H_9 potential energy surface. Given the complexity of the reaction surface, and the very wide range of reaction conditions that need to be considered, it is to be expected that the predicted products and rate coefficients will depend strongly on the specific reaction conditions. In this paper, we limit ourselves to discussing the most important pathways, identifying interesting competitions between reaction channels while indicating the expected changes in the relative importance of these competing channels upon varying the temperature and pressure, and looking for the most likely product channels. Results for specific reaction conditions can be found in the papers discussing the final RRKM-ME calculations in detail.[29,30]

II. Methodology

The geometries of the reactants, products, various intermediates, and transition states of importance in the title reaction were optimized using the hybrid density functional B3LYP-DFT method, i.e., Becke's three-parameter nonlocal exchange functional[42] combined with the nonlocal correlation functional of Lee, Yang, and Parr.[43] These computations were performed using the Gaussian quantum chemical program.[44] Due to the extreme complexity of the potential energy surface, we restricted ourselves to the investigation of 75 minima and 157 transition structures (TSs). These stationary points were selected on the basis of theoretical-kinetic RRKM-Master equation (RRKM-ME) calculations,[29] which were performed in tandem with the quantum chemical calculations: each time a new relevant intermediate was found, its unimolecular reactions were also characterized and inserted into the RRKM-ME calculations; any subsequent reactions of the products of these new reactions were only examined in detail if they themselves were also formed with a sufficiently large probability. This approach enabled us to identify the reaction channels that contribute significantly, and to ignore reactions of intermediates that do not affect the product formation appreciably. The goal was to recover over 99% of the product formation; i.e., less than 1% of the reaction flux passes through unexplored parts of the PES. The considered temperatures in these RRKM-ME calculations were 20−4000 K, with pressures from 10^{-9} to 10^{8} Pa. These wide ranges ensure that all relevant reaction conditions, i.e., from the cold low-pressure conditions inside dark stellar clouds, over high-pressure combustion systems, to very high temperature conditions in the outflow of carbon stars, are considered and can be adequately described in the later RRKM calculations.[29,30]

The geometry optimizations were first performed using the 6-31G(d) basis set. The harmonic vibrational frequencies, evaluated analytically, identified all stationary points as minima or transition states. The geometry optimization was then repeated for most structures using the 6-311+G(d,p) basis set. Relative energies for the minima and TSs are listed in Table 1. The convergence of the B3LYP-DFT results with respect to the basis set is quite good, as the average difference between the 6-31G(d) and 6-311+G(d,p) relative energies for the 68 characterized intermediates is 5.8 kJ mol^{-1}. As can be expected, the average relative energy of the transition states (numbering 127 TSs) drops slightly by 4.1 kJ mol^{-1} due to the larger basis set, also with a scatter of 5.5 kJ mol^{-1}. Most of the scatter is due to high-energy isomers and TSs that tend to be less important in kinetic considerations. The relative energies of the separated products are more sensitive to the basis set used, due to basis set superposition errors (BSSEs); fortunately, these higher uncertainties do not influence kinetic calculations, since the rate of product formation is determined by the characteristics of the dissociation TSs. Due to the computational expense, we decided not to perform IRC calculations on all transition-state structures. We did visualize all the transition-state geometries and the movement corresponding to the reaction mode (i.e., the vibrational mode with an imaginary frequency). In nearly all cases, this allowed us to clearly identify which minima the transition state connects; for some TSs we performed additional calculations (partial geometry optimizations) to verify that a well-behaved reaction path is available between the TS and the equilibrium geometry of the reactant/product.

The heights of the barriers for the initial reaction with respect to the energy of phenyl + C_3H_4 have an impact both on the predicted absolute rate coefficient and on the relative importance of the different entrance channels. Higher level single-point QCISD(T)/6-311G(d,p) and CCSD(T)/6-311G(d,p) calculations on the B3LYP-DFT/6-31G(d) and B3LYP/6-311+G(d,p) geometries were therefore performed to pursue reliable estimates of these barrier heights.[45] For the open-shell radicals a spin unrestricted reference was used, UHF-QCISD(T) and UHF-CCSD(T) as implemented in Gaussian 98,[44] as well as the partially spin restricted formalism derived by Knowles et al.[46] for the coupled cluster approach, i.e., RHF-RCCSD(T).[47] The latter computations were performed with the MOLPRO system of programs.[48] The Hartree−Fock core orbitals were kept frozen in all correlated computations. The energetic results are listed in Table 2, including ZPE-corrected relative energies, using the harmonic wavenumbers obtained at both the B3LYP/6-31G(d) and B3LYP/6-311+G(d,p) levels of theory. These results confirm that tsrad1_Ph+propyne is the entrance channel with the lowest barrier, 14 kJ mol^{-1}; the second addition channel tsrad4_Ph+propyne has a barrier about 5 kJ mol^{-1} higher in energy (19 kJ mol^{-1}). For hydrogen transfers, DFT is known[49−53] to underestimate the barrier heights by up to 15 kJ mol^{-1}; the CCSD(T) and QCISD(T) results of approximately 21 kJ mol^{-1} will be used for kinetic calculations. We also attempted G2(B3LYP/MP2) and G2(B3LYP/MP2/CC) calculations, but these suffered from severe spin contamination problems in the UHF-MP2 calculations ($\langle S^{**}2\rangle$ up to 1.56), making these calculations less reliable even though they agree with the results in Table 2 within 3−5 kJ mol^{-1}.

Several of the structures characterized have one or more degrees of freedom for internal rotation, which lead to different conformers. For future kinetic calculations, the degrees of freedom for internal rotation would be described better as (hindered) internal rotors, especially in view of the high internal energy of the intermediates. We therefore opted not to characterize all rotamers of each isomer; rather, we identified the harmonic vibrational modes in the quantum chemical frequency analysis corresponding to such internal rotations, and will

(42) Becke, A. D. *J. Chem. Phys.* **1992**, *97*, 9173.
(43) Lee, A.; Yang, W.; Parr, R. G. *Phys. Rev. B* **1988**, *37*, 785.
(44) Gaussian 98, revision A.5: Frisch, M. J., et al., Gaussian Inc., Pittsburgh, PA, 1998.
(45) Pople, J. A.; Head-Gordon M.; Raghavachari, K. *J. Chem. Phys.* **1987**, *87*, 5968.
(46) Knowles, P. J.; Hampel, C.; Werner, H.-J. *J. Chem. Phys.* **1993**, *99*, 5219; **2000**, *112*, 3106 (erratum).
(47) Watts, J. D.; Gauss, J.; Bartlett, R. J. *J. Chem. Phys.* **1993**, *98*, 8718.
(48) MOLPRO is a package of ab initio programs written by H.-J. Werner and P. J. Knowles, with contributions from Amos, R. D.; Bernhardsson, A.; Berning, A.; Celani, P.; Cooper, D. L.; Deegan, M. J. O.; Dobbyn, A. J.; Eckert, F.; Hampel, C.; Hetzer, G.; Korona, T.; Lindh, R.; Lloyd, A. W.; McNicholas, S. J.; Manby, F. R.; Meyer, W.; Mura, M. E.; Nicklass, A.; Palmieri, P.; Pitzer, R.; Rauhut, G., Schütz, M.; Stoll, H.; Stone, A. J.; Tarroni, R., and Thorsteinsson, T., version 2000.1.
(49) Johnson, B. G.; Gonzales, C. A.; Gill, P. M. W.; Pople, J. A. *Chem. Phys. Lett.* **1994**, *221*, 100.
(50) Durant, J. L. *Chem. Phys. Lett.* **1996**, *256*, 595.
(51) Lynch, B. J.; Truhlar, D. G. *J. Phys. Chem. A* **2001**, *105*, 2936.
(52) Basch, H.; Hoz, S. *J. Phys. Chem.* **1997**, *101*, 4416.
(53) Nguyen, M. T.; Creve, S.; Vanquickenborne, L. G. *J. Chem. Phys.* **1996**, *105*, 1922.

Table 1. ZPE-Corrected Relative Energies Relative to That of Indan-1-yl (RAD23) for the [C_9H_9] Potential Energy Surface[a]

compd	E_{rel} (kJ mol^{-1})	compd	E_{rel} (kJ mol^{-1})	compd	E_{rel} (kJ mol^{-1})	compd	E_{rel} (kJ mol^{-1})
phenyl + propyne	281.9	RAD47	359.3	tsPh+propyne_benzene+2-propynyl	293.9	tsrad18rad59	325.1
phenyl + allene	274.6	RAD48	479.6	tsrad1_Ph+propyne	299.0	tsrad18rad60syn	305.4
Ph + cyclo-C_3H_4	384.4	RAD49	460.6	tsrad1_PhCCCH$_3$+H	284.0	tsrad18rad60anti	308.0
benzene + 2-propynyl	199.4	RAD50	251.7	tsrad1_PhCHCCH$_2$+H	281.5	tsrad19_PhcycC$_3$H$_4$	393.4
PhCHCCH$_2$ + H	276.2	RAD51	237.0	tsrad1rad2	141.3	tsrad19syn_PhcycC$_3$H$_3$_A+H	385.2[b]
PhCCCH$_3$ + H	269.9	RAD52	311.5	tsrad1rad5	321.2	tsrad19syn_PhcycC$_3$H$_3$_B+H (elimination of *syn*-H)	400.9[b]
PhCCH + CH$_3$	225.9	RAD47	359.3	tsrad1rad9	297.8	tsrad18rad59	325.1
PhcycC$_3$H$_3$_A+H	364.7	RAD53	197.5	tsrad2_PhCCCH$_3$+H	284.2	tsrad19syn_PhcycC$_3$H$_3$_B+H (elimination of *anti*-H)	405.2[b]
PhcycC$_3$H$_3$_B+H	386.8	RAD54	290.4	tsrad2_PhCHCCH$_2$+H	280.9	tsrad19anti_PhcycC$_3$H$_3$_A+H	385.2[b]
PhCH$_2$CCH + H	311.0	RAD55	277.2	tsrad2rad8	291.3	tsrad19anti_PhcycC$_3$H$_3$_B+H (elimination of *syn*-H)	400.9[b]
PhC(CH3)C| + H	491.1	RAD56	398.4	tsrad2rad10	242.8	tsrad19anti_PhcycC$_3$H$_3$_B+H (elimination of *anti*-H)	405.2[b]
PhC(H)C| + CH$_3$	452.1[b]	RAD57	474.3	tsrad2rad27	269.4	tsrad19synanti	185.2
C$_2$H$_2$ + PhCH$_2$	201.8	RAD59	309.3	tsrad2rad31	249.2	tsrad20_C$_2$H$_2$+PhCH$_2$	258.3
PAH1 + H	374.8	RAD60syn	154.7	tsrad3_PhCCH+CH$_3$	283.2	tsrad20_PhCH$_2$CCH+H	326.4
indene + H (PAH2 + H)	175.5	RAD60anti	189.8	tsrad3rad4	167.6	tsrad20rad21	216.7
PAH3 + H	315.8	RAD61	364.8	tsrad3rad13	252.2	tsrad21rad22	219.0
PAH4 + H	649.2[b]	RAD62	230.6	tsrad3rad14	278.6	tsrad21rad24	231.7
PAH7 + H	297.5	RAD63	515.2[b]	tsrad3rad31	251.8	tsrad22_indene+H	185.2
PAH8 + H	445.4[b]	RAD64	352.8	tsrad4_Ph+propyne	310.1	tsrad22rad23	191.7
PAH9 + H	264.1	RAD66	307.5	tsrad4rad5	371.7	tsrad23_indene+H	175.5
PAH10 + CH$_3$	331.5	RAD67	307.5	tsrad4rad6	302.0	tsrad23_PAH9+H	266.9[b]
PAH11 + H	292.5	RAD68syn	236.5	tsrad5_PhCCCH$_3$+H	276.6	tsrad23rad35	262.4
PAH12 + H	437.5	RAD68anti	216.0	tsrad5_PhCCH+CH$_3$	253.9	tsrad23rad36	163.7
PAH14 + H	386.2	RAD70	289.4	tsrad5rad8	297.6	tsrad23rad65	361.4
RAD1	132.0			tsrad5rad10	336.3	tsrad24_PAH7+H	314.6
RAD2	122.8			tsrad5rad12	339.7	tsrad24rad25	335.1
RAD3	153.4			tsrad6_Ph+allene	301.9	tsrad24rad26	323.9
RAD4	155.9			tsrad6rad7	223.6	tsrad24rad28	305.7
RAD5	100.3			tsrad6rad13	218.2	tsrad24rad45	195.4
RAD6	51.7			tsrad6rad29	208.3	tsrad25_PAH7+H	320.6
RAD7	125.0			tsrad6rad33	237.6	tsrad25_PAH8+H_syn	443.6[b]
RAD8	17.9			tsrad7_PhcycC$_3$H$_3$_A+H	369.1[b]	tsrad25_PAH8+H_anti	447.5[b]
RAD9	34.8			tsrad7rad19	343.9	tsrad25rad33	385.3
RAD10	144.5			tsrad8_PhCHCCH$_2$+H	284.9	tsrad25rad34	376.2
RAD11	148.6			tsrad8rad9	66.5	tsrad25rad40syn	435.8
RAD12	150.6			tsrad8rad19	235.9	tsrad25rad40anti	441.7
RAD13	153.9			tsrad8rad20	304.4	tsrad25rad68syn	418.4
RAD14	212.1			tsrad8rad21	314.6	tsrad25rad68anti	418.4
RAD15	83.9			tsrad9_PhCHCCH$_2$+H	284.9	tsrad25rad70	364.3
RAD16	344.4[b]			tsrad9rad11	295.5	tsrad26_PAH1+H	379.7[b]
RAD17	461.6[b]			tsrad9rad12	177.3	tsrad26_PAH10+CH$_3$	354.4[b]
RAD18	118.9			tsrad9rad15	177.0	tsrad26rad27	370.3
RAD19syn	180.4			tsrad9rad19	232.4	tsrad26rad28	313.2
RAD19anti	183.1			tsrad9rad21	314.9	tsrad26rad37	311.4
RAD20	168.4			tsrad10rad26	272.6	tsrad26rad38	338.6
RAD21	173.1			tsrad11_Ph+allene	291.4	tsrad26rad61	411.6
RAD22	42.3			tsrad11_PhCHCCH$_2$+H	289.8	tsrad27_PAH1+H	383.2
RAD23 (indan-1-yl)	0.0			tsrad11_PhCH$_2$CCH+H	317.0	tsrad27_PAH8+H	442.5[b]
RAD24	164.0			tsrad11rad20	349.7	tsrad27rad40anti	431.7
RAD25	215.8			tsrad11rad21	247.8	tsrad27rad40syn	431.5
RAD26	130.6			tsrad11rad25	276.5	tsrad27rad41	382.7
RAD27	209.4			tsrad11rad29	235.1	tsrad27rad43	350.8
RAD28	114.2			tsrad12rad26	298.3	tsrad28_PAH1+H	375.4[b]
RAD29	208.4			tsrad13rad28	271.5	tsrad28_PAH7+H	299.3[b]
RAD30	68.6			tsrad14_PAH1+H	384.5	tsrad28rad39	300.5
RAD31	242.9			tsrad14rad27	392.7	tsrad28rad64	400.1
RAD32	81.5			tsrad14rad28	366.2	tsrad29rad49	486.9
RAD33	190.9			tsrad14rad33	553.4	tsrad30_indene+H	187.6
RAD34	179.5			tsrad14rad42	381.5	tsrad31rad48	498.2
RAD35	186.8			tsrad14rad62	354.6	tsrad33_PAH7+H	315.3
RAD36	66.0			tsrad15_indene+H	194.5	tsrad33rad53	397.4
RAD37	320.2			tsrad15rad18	278.6	tsrad33rad54	350.4
RAD38	251.4			tsrad15rad35syn	310.6	tsrad33rad55	365.8
RAD39	236.5			tsrad15rad35anti	315.0	tsrad33rad56	415.2
RAD40anti	307.4			tsrad15rad67	311.8	tsrad36rad38	268.3
RAD40syn	303.9			tsrad18_indene+H	203.4	tsrad36rad45	71.9
RAD41	245.2			tsrad18_PAH3+H	328.7[b]	tsrad36rad47	373.6
RAD42	247.7			tsrad18rad20	221.5	tsrad36rad51	354.5
RAD43	230.0			tsrad18rad22	223.8	tsrad36rad52	342.1
RAD44	500.1			tsrad18rad30	272.1	tsrad39rad45	347.4
RAD45	59.8			tsrad18rad35syn	318.9	tsrad45rad46	286.5
RAD46	218.2			tsrad18rad35anti	327.4	tsrad45rad47	371.7

[a] See Figures 1 and 2 for labeling, and the Supporting Information for absolute energetic data and more information. [b] Calculated using the B3LYP-DFT/6-31G(d) energy.

Table 2. Energies (hartrees) of the Entrance Transition States at Different Levels of Theory (Single-Point Calculations on B3LYP-DFT Geometries)[a]

	B3LYP-DFT/ 6-31G(d)[b] UQCISD(T)/ 6-311G(d,p)[c]		B3LYP-DFT/ 6-31G(d)[b] UCCSD(T)/6 -311G(d,p)[c]		B3LYP-DFT/ 6-311+G(d,p)[b] RCCSD(T)/6 -311G(d,p)[c]	
structure	energy	E_{rel}	energy	E_{rel}	energy	E_{rel}
phenyl + propyne	−347.32673	0.0	−347.32577	0.0	−347.32826	0.0
tsrad1_Ph+propyne	−347.32207	13.3	−347.32072	14.3	−347.32300	14.5
tsrad4_Ph+propyne	−347.32026	18.4	−347.31879	19.7	−347.32131	19.4
TS H abstraction[d]	−347.31494	20.5	−347.31374	21.1	−347.31626	21.4

[a] E_{rel} are the ZPE-corrected relative energies (kJ mol^{-1}), using the vibrational wavenumbers obtained at the same level of theory as the geometry optimization. [b] Geometry and ZPE. [c] Single-point method. [d] Phenyl + propyne → benzene + 2-propynyl.

treat these modes with a more appropriate model for describing hindered internal rotors.

Some of the dissociation pathways (e.g., tsrad23_indene+H) do not have an exit barrier and therefore cannot be described by conventional transition-state models in the kinetic calculations. Rather, these barrierless reactions (see also Table 1) need a microvariational treatment, in which the energy-dependent internal-states-minimum bottleneck for reaction is found on the basis of an optimization using the complete description of the molecular properties, i.e., rovibrational data and the potential energy profile along the reaction coordinate. Similar to earlier work on barrierless reactions,[54,55] this can be done by a number of constrained optimizations at varying C−H bond lengths, followed by a frequency analysis on each point, which obviously is computationally very demanding. Fortunately, all but one of the barrierless exit channels are quite high in energy and therefore probably carry a negligible reaction flux. For these TSs we optimized only one point along the reaction coordinate, for a C−H bond length between 2.0 and 2.5 Å (see the Supporting Information), and used the corresponding data to calculate the rate constants. The energy-specific rate coefficients obtained in this manner always[56] overestimate the rate coefficients that would be obtained in a complete microvariational treatment to identify the true bottleneck for reaction; hence, if the reaction flux is negligible using this one-point approximation, it should be even more so in a full microvariational treatment. For tsrad23_indene+H, which carries a significant reaction flux, we did perform constrained geometry optimizations at intervals of 0.1 Å along the reaction coordinate, up to a C−H bond length of 4 Å, and calculated the frequencies for each point, projecting out the reaction coordinate mode to avoid mixing with the vibrational modes.

III. Results and Discussion

The ZPE-corrected relative energies of the reactants, products, intermediates, and transition states relevant for the phenyl + propyne reaction are listed in Table 1. The reaction scheme is depicted in Figure 1, while a simplified version of the PES showing only the reaction pathways leading to the most important products is shown in Figure 2. The complete set of quantum chemical data may be found in the Supporting Information, including the Lewis structure representations of all intermediates; the most important C_9H_9 isomers and reaction pathways are depicted in Figure 2. The intermediates are labeled as RAD*x*, with *x* an ordinal number, while the transition states are named after the two minima connected: ts*xy* connects intermediate *x* with intermediate/product *y*. Dissociated reaction products containing a bicyclic structure are labeled as PAH*x*, with *x* an ordinal number, irrespective of whether the bicyclic structure is actually aromatic. As already mentioned, only the kinetically important part of the PES was characterized. RRKM-Master equation calculations[29] performed at a very wide range of temperatures and pressures served to identify the intermediates through which the reactive flux is negligibly small. These intermediates are frozen, as indicated by an "×" in Figure 1, and no effort was done to investigate further reactions of these intermediates. The aim was to predict 99% of the product formation correctly; i.e., only 1% of the reactive flux ends up as "frozen intermediate". Note that the current selection of frozen intermediates is only valid for the phenyl + propyne reaction; if a different entry point into the $[C_9H_9]$ PES is taken, it may be necessary to take the reactions of some of the currently frozen intermediates into account. It should be stressed that this paper does not involve a detailed, quantitative account of the reaction kinetics of this reaction; the RRKM-ME results given here can be used to provide some qualitative insight into the complex mechanism, identifying the most important reactions, intermediates, and products, which are discussed below, and to ensure that the quantum chemical characterization spans a sufficiently large part of the PES to allow later quantitative theoretical-kinetic calculations for all relevant reaction conditions.

Occasionally, the B3LYP/6-31G(d) calculations showed that some transition states were much too high in energy to compete, or that the product of a reaction was too high in energy for the TS to be competitive; in these cases (indicated by dashed arrows in Figure 1) no further calculations were done on the reaction path. We include our rationalization for each of these structures in the Supporting Information.

A. Initial Reaction of Phenyl with Propyne. Three pathways are accessible for the initial reaction of phenyl with propyne: two addition reactions on the carbons on either side of the triple bond, and a hydrogen transfer from propyne to phenyl. The H transfer of a methyl hydrogen proceeds over a barrier of 21 kJ mol^{-1} (average of the ZPE-corrected QCISD(T) and CCSD(T) results in Table 2), forming 2-propynyl and benzene with a reaction exoergicity of 82.5 kJ mol^{-1}. Hydrogen abstraction of the acetylenic hydrogen can be neglected under all reaction conditions: 1-propynyl ($CCCH_3$) is 181 kJ mol^{-1} less stable than 2-propynyl,[54] such that this reaction is strongly endoergic by about 100 kJ mol^{-1} and therefore not competitive. Addition of phenyl to the outer acetylenic carbon in propyne, leading to radical RAD1, is the most favorable route energetically, with a barrier of 14 kJ mol^{-1} (Table 2). Note that isomerization between RAD1 and RAD2 (the *Z*- and *E*-conformers of the initial adduct) via tsrad1rad2 always is a rapid process due to the excess internal energy available in the adduct imparted by the reaction exoergicity and to the low isomerization barrier (less than 20 kJ mol^{-1}). The ratio RAD1/RAD2 will therefore always go to a microcanonical equilibrium, so that explicit consideration of the conformer formed in the initial reaction is

(54) Vereecken, L.; Pierloot, K.; Peeters, J. *J. Chem. Phys.* **1998**, *108*, 1068.
(55) Vereecken, L.; Peeters, J. *J. Phys. Chem. A* **1999**, *103*, 5523.
(56) Holbrook, K.; Pilling, M.; Robertson, S. *Unimolecular Reactions*, 2nd ed.; Wiley: New York; 1996.

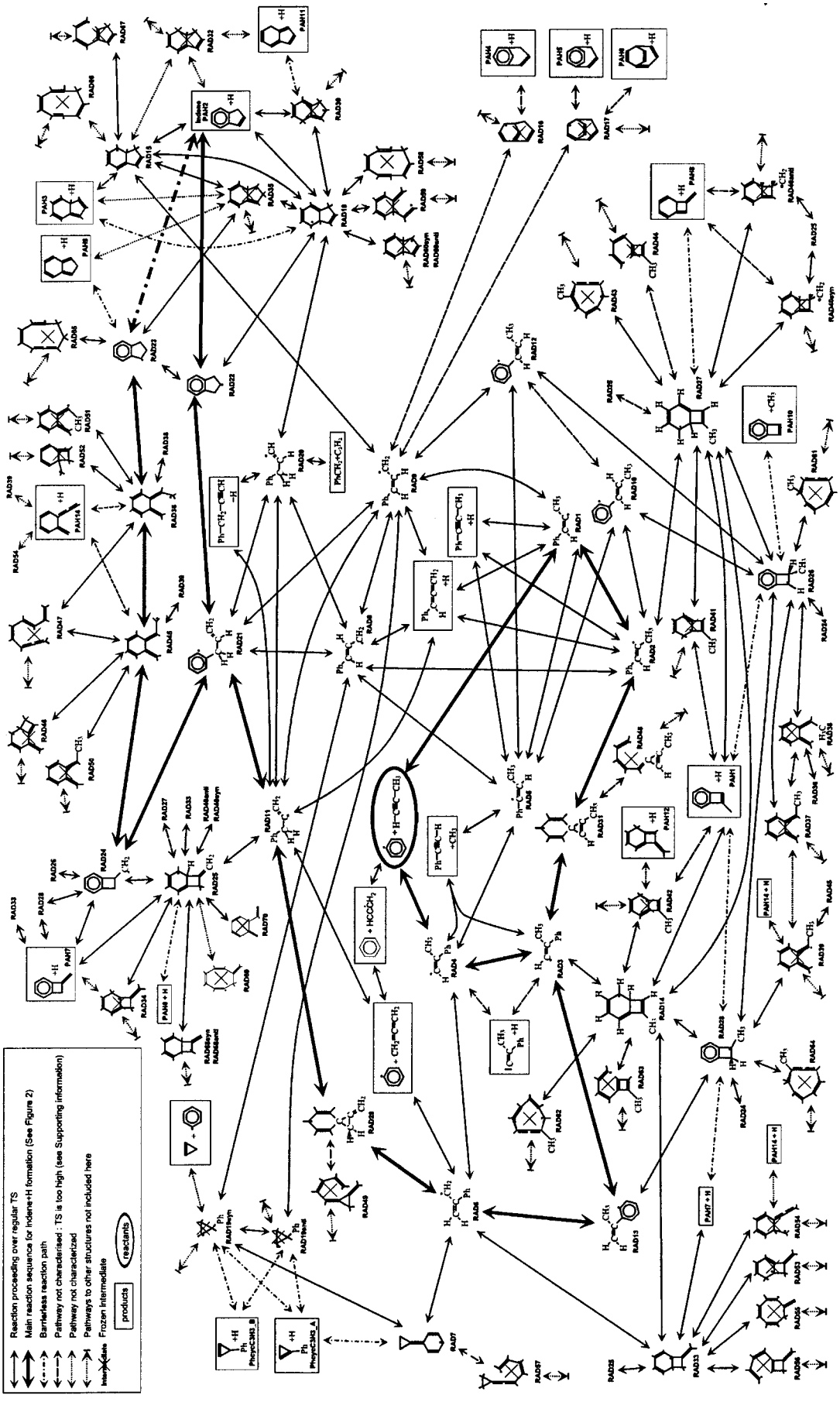

Figure 1. Reaction scheme for the phenyl + propyne reaction.

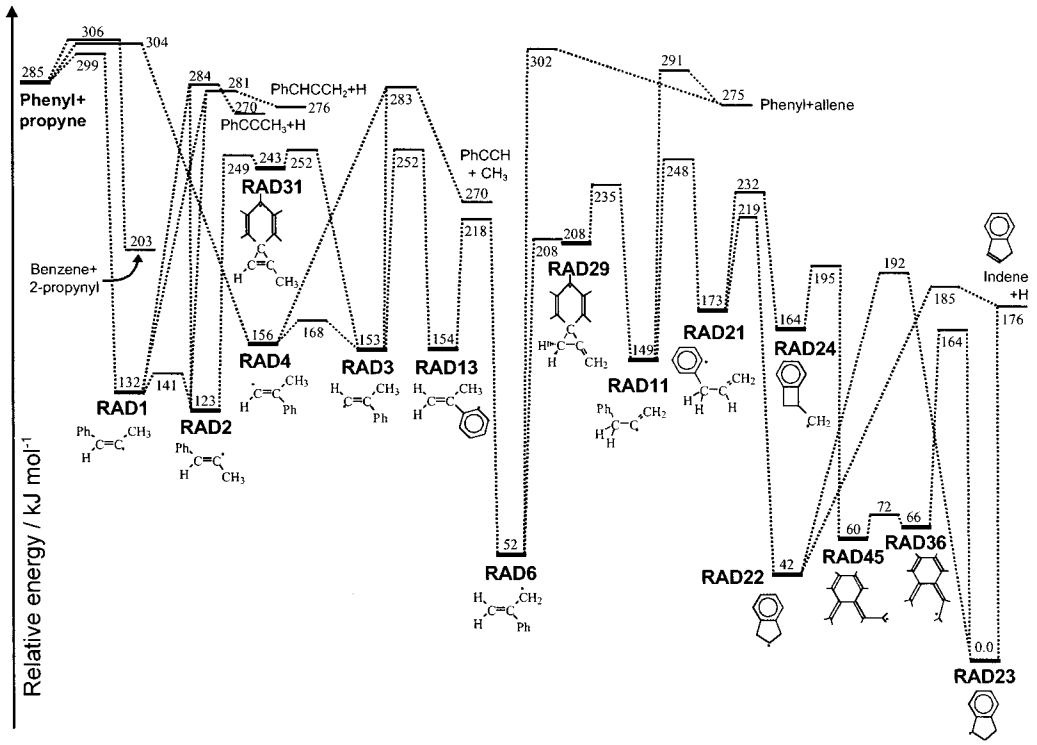

Figure 2. Selected reactions of the activated intermediates in the phenyl + propyne reaction, showing formation of indene + H, as well as the most important other dissociation channels to $PhCCCH_3$ + H, $PhCHCCH_2$ + H, and PhCCH + CH_3. The reactions in this scheme are not sufficient for accurate kinetic analysis of the phenyl + propyne reaction. The energies are the ZPE-corrected B3LYP-DFT/6-311+G(d,p) data, except for the entrance channels, which are based on Table 2.

not needed. Addition to the central carbon of propyne via tsrad4–Ph+propyne has a slightly higher entrance barrier of 19 kJ mol^{-1}, similar in height to the hydrogen abstraction. Again, the *Z*- and *E*-conformers of the adduct, RAD4 and RAD3, can quickly interconvert through tsrad3rad4.

The relative barrier heights for the three entrance channels suggest that tsrad1–Ph+propyne will be the most favorable transition state at lower temperatures. At higher temperatures, the other two channels will increase in importance, but since the difference in energy with the lowest TS is fairly small, less than 10 kJ mol^{-1}, the relative rigidity of the transition states will also affect the temperature at which the other entrance channels become competitive with tsrad1–Ph+propyne. Tunneling could be an important contributor to the H-transfer reaction rates at low to intermediate temperatures.

More exotic reaction channels, such as S_N2-like Ph/H substitution reactions leading directly to $PhCH_2CCH$ + H, all have much higher barriers to reaction, and need not be considered.

B. Unimolecular Reactions of the Activated Intermediates. Preliminary RRKM-ME calculations[29] show that, especially at lower temperatures, most, if not all, of the activated adducts leave the direct route from initial adduct to product at some point during their lifetime and venture into the less important parts of the PES, only to return to the main reaction channels later. Due to the complexity of the reaction surface, not all of these isomerization pathways can be discussed in detail, so we will focus here mainly on the most important product formation pathways. These main pathways are shown in the simplified PES, as depicted in Figure 2. These are only the most important channels; consideration of the full PES is necessary to properly describe the quantitative temperature and pressure dependence of the product distribution of this reaction. As most of the side channels leave the activated molecules no egress, they must return to the main channel by one pathway or another. These side steps affect the lifetime of the intermediate and the number of times it passes through an isomeric state that allows dissociation through a low-lying exit channel.

The first interesting isomerization is the RAD2 ↔ RAD31 ↔ RAD3 sequence, a phenyl shift which allows interconversion of the initial adducts formed in the two addition channels.

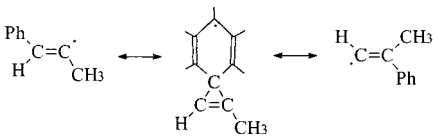

Because of the delocalization of the free electron over the benzene ring, the transition states are fairly low in energy, about 30 kJ mol^{-1} below the competing dissociation channels. At higher temperatures, where the initial adducts have a substantial amount of internal energy, reaction over the tight isomerization transition states must compete with the dissociation channels, which involve higher energy but looser transition states. This will be discussed later. A hydrogen or methyl shift connecting RAD1/RAD2 and RAD3/RAD4 through RAD5 (see Figure 1) is energetically much more difficult than the phenyl shift, even though intermediate RAD5 itself is quite stable, lying 30 kJ mol^{-1} below RAD1.

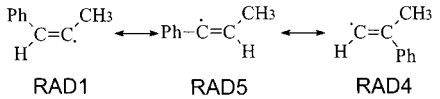

Most of this stability of RAD5 is due to the delocalization of the unpaired electron in the conjugated system spanning the benzene π-system and the radical p-orbital of the unsubstituted carbon; this requires a perpendicular orientation of the phenyl group with respect to the double bond. Such delocalization is absent in the transition states for H or for CH_3 shift, which penalizes these TSs energetically and renders them of little importance kinetically compared to the phenyl shift: the highest transition state in the sequence RAD1 ↔ RAD5 ↔ RAD4, tsrad4rad5, is about 120 kJ mol^{-1} above the highest transition state when going over RAD31.

There are a number of dissociation transition states starting from the initial adducts RAD1, RAD2, RAD3, and RAD4, all about 20 kJ mol^{-1} below the entrance transition states (see Figure 2). These lead to substituted acetylenes or allenes: $PhCCCH_3$ + H, $PhCHCCH_2$ + H, and PhCCH + CH_3. The dissociation transition states are fairly loose, and will be the main exit channels at higher temperatures. At low temperatures, however, the adducts have less internal energy, and reaction through the tighter but energetically more favorable isomerization transition states will be competitive.

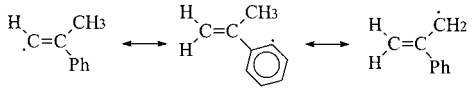

Formation of RAD13 from RAD3 is the most important of these competing isomerization channels, tsrad3rad13 is about as high as those in the RAD2 ↔ RAD31 ↔ RAD3 sequence, followed by isomerization of RAD13 to the low-lying RAD6 intermediate, which is strongly stabilized by allyl-type resonance. Direct isomerization of RAD4 to RAD6 is less likely due to the high barrier, with tsrad4rad6 similar in energy to the entrance transition states. There are also a large number of side channels, leading to bicyclic [4.2.0] structures such as RAD14, RAD27, RAD33, ..., but the hydrogen elimination exit channels from these intermediates lead to nonaromatic or even antiaromatic [4.2.0] bicyclic structures (H + PAH1, PAH8, PAH10, PAH12, ...) that therefore are energetically not accessible. (Nearly) all intermediates that venture into this part of the PES will return to the isomeric forms of the main reaction sequence outlined above. The RAD6 ↔ RAD29 ↔ RAD11 reaction sequence, essentially a phenyl shift, followed by a hydrogen shift to RAD21, is crucial for the low-temperature product distribution of the phenyl + propyne reaction, since it is among the most energy demanding steps in the formation of indene + H (see Figure 2).

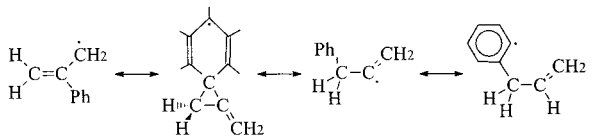

The rate-limiting step for this sequence, transition state tsrad11rad21, is 51 kJ mol^{-1} below the entrance transition state tsrad1–Ph+propyne. Note that both RAD6 and RAD11 can dissociate into phenyl + allene, though the high exit barriers make these less important exit channels.

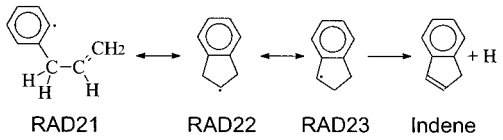

Once RAD21 is formed, the reaction proceeds mainly by facile ring closure to RAD22 followed either by direct dissociation into indene + H or by isomerization to RAD23 and subsequent dissociation into indene + H. The exit channel leading to indene is accessible to all chemically activated intermedates formed in the initial reaction, as all isomerization TSs and the dissociation transition state are below the energy level of the reactants Ph + CH_3CCH. About a quarter of the intermediates follow a side channel RAD21 ↔ RAD24 ↔ RAD45 ↔ RAD36 ↔ RAD23 (see Figure 2) but still dissociate to indene + H.

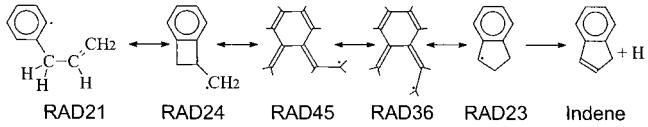

Dissociation of the planar RAD23 (indan-1-yl), the most stable C_9H_9 intermediate characterized, to the aromatic indene + H product proceeds without exit barrier; the evolution of energy, moments of inertia, and vibrational wavenumbers along the reaction coordinate was obtained as outlined in the Methodology Section. The detailed numerical results and some graphical representations may be found in the Supporting Information.

C. Additional Reaction Channels. A large number of the pathways depicted in Figure 1 carry only a small percentage of the reaction flux of the phenyl + propyne reaction; therefore, these are less important in describing the reaction. However, the PES characterized here will also be used in the theoretical-kinetic study of other reactions proceeding over the [C_9H_9] PES, e.g., phenyl + allene, phenyl + cyclo-C_3H_4, and $PhCH_2$ + C_2H_2, where it is possible that reaction channels less important in the phenyl + propyne reaction become accessible.

The reaction of phenyl with cyclopropene will form the RAD19 intermediate initially (both syn- and anti-conformers were characterized). This should break the three-membered ring easily since the barrier to form the resonance-stabilized RAD8 and RAD9 intermediates is only 60 kJ mol^{-1}. Formation of substituted cyclopropenes from RAD19 through barrierless reactions cannot compete with the ring opening. The barrier for interconversion of the *Z*- and *E*-conformers RAD9 and RAD8 is only 30−50 kJ mol^{-1}, such that explicit consideration of the syn- or anti-forms in the preceding reactions is of less importance due to rapid instatement of a microcanonical equilibrium. The energy released by the breaking of the three-membered ring permits rapid ring closure to RAD15, a bicyclic [4.3.0] structure that can subsequently dissociate to indene + H. Some isomerization to other bicyclic [4.3.0] structures might occur, but all low-energy pathways ultimately lead to dissociation and indene + H as the reaction products.

The $PhCH_2$ + C_2H_2 reaction leads to RAD20, which can either undergo an H shift leading to RAD11 or RAD21 (intermediates that were discussed earlier) or undergo ring closure to RAD18. The most likely dissociation channel for all

of these intermediates is the formation of indene + H, even if some isomerization to other C_9H_9 isomers occurs prior to dissociation.

IV. Conclusions

Three reaction channels have been identified for the phenyl + propyne reaction: two addition reactions, one on each of the two acetylenic carbons, and a hydrogen abstraction leading directly to benzene + 2-propynyl (propargyl). The reaction of phenyl radicals with propyne proceeds over a complex PES, which has been characterized here at the B3LYP-DFT level of theory for application in future theoretical-kinetic studies[29] on the reaction rate and the product distribution. Higher level quantum chemical computations have been performed on the entrance transition states and the reactants to allow for a more reliable prediction of the absolute rate coefficient of phenyl + propyne. Reaction channels leading to substituted acetylenes and allenes, including PhCCH, $PhCCCH_3$, and $PhCHCCH_2$, have also been characterized. The lowest energy pathway, however, leads to the aromatic bicyclic indene, a prototype PAH molecule containing a five-membered ring. The formation of indene starting from RAD1 as formed in the energetically most favorable entrance channel requires a sequence of at least 10 isomerizations. The highest reaction barrier in this sequence is 60 kJ mol^{-1} below the lowest entrance barrier, such that this pathway is accessible to all initially formed chemically activated intermediates, even at the lowest temperatures.

While the importance of the phenyl + propyne and similar reactions on PAH formation can only be assessed after the theoretical-kinetic calculations on rate coefficients and product distributions have been completed, and these results have been incorporated into modeling studies, some important observations can already be made. The barrier to reaction for phenyl radicals + propyne is of a height comparable to that for other alkenes and alkynes, such as acetylene, so it is expected that the rate coefficients of these reactions will be of similar order of magnitude. In combustion systems, acetylene is often present in quite high concentrations, but contributions from a number of unsaturated species with an odd number of carbons could sum to a significant additional PAH-growth channel. For the interstellar medium, where C_3H_x species are among the most abundant organic molecules observed, reactions of phenyl radicals with unsaturated C_3H_x ($x = 1-3$) species similar to the title reaction might outrun PAH-growth processes involving acetylene, especially at very low temperatures where the reaction barriers for coreactants such as acetylene and propyne lead to very slow reaction rates. As the formation of indene + H is energetically accessible to all initially formed C_9H_9 intermediates, phenyl + C_3H_4 is potentially a direct source of bicyclic hydrocarbons at all temperatures. Other possible products of this reaction are substituted acetylenes and allenes, and stabilized C_9H_9 radicals at higher pressures. The exact product distribution will obviously depend on temperature and pressure, but each of these compounds is interesting in its own respect in the context of PAH growth, as the reactive, unsaturated tail connected to the phenyl group allows for facile subsequent addition reactions, possibly followed by ring closure. The (possible) presence of aliphatic hydrogens, which have weaker bonds than olefinic hydrogens, can facilitate similar further reactions initiated by H abstraction.

From this, we conclude that the addition of aromatic radical units to unsaturated, nonacetylene hydrocarbons has the potential to be an important channel for PAH growth, supplementing the rate of PAH growth through the traditional, acetylene-based reaction mechanisms. The addition of the aromatic radicals to unsaturated molecules bearing an odd number of carbons could lead to the direct formation of polycyclic hydrocarbons containing five-membered rings. The potential energy surface as calculated for the phenyl + propyne reaction indicates that the pathways leading to interesting reaction products can be very complex, even if they are energetically the most favorable, making the study of these reactions a true challenge.

Acknowledgment. J.P. and L.V. thank the Fund for Scientific Research Flanders (FWO-Vlaanderen) and the KULeuven Research Council (PDM and BOF Fund) for continuing support. H.F.B. thanks the Fonds der Chemischen Industrie for a Liebig Fellowship and Professor W. Sander for encouragement. The work at the University of Georgia was supported by the U.S. Department of Energy Combustion and SciDAC research programs. The U.S. Department of Energy provided support in Athens and at the Deutsche Forschungsgemeinschaft at Erlangen.

Supporting Information Available: Additional notes on the quantum chemical calculations, including the treatment of the barrierless reaction channels, Lewis structure representations for the intermediates, and the complete set of DFT energies, point groups, Cartesian coordinates, rotational constants, vibrational wavenumbers, and ZPE corrections. This material is available free of charge via the Internet at http://pubs.acs.org. It can also be downloaded from the author's Web site (http://arrhenius.chem.kuleuven.ac.be) or obtained directly from the author.

JA017018+